Monthly Notices
of the
ROYAL ASTRONOMICAL SOCIETY

MNRAS **458,** L69–L73 (2016) doi:10.1093/mnrasl/slw019
Advance Access publication 2016 February 19

Radio-loud Narrow Line Seyfert 1 under a different perspective: a revised black hole mass estimate from optical spectropolarimetry

Ranieri D. Baldi,[1,2]★ Alessandro Capetti,[3] Andrew Robinson,[4] Ari Laor[2] and Ehud Behar[2]

[1]*Department of Physics and Astronomy, University of Southampton, Southampton SO17 1BJ, UK*
[2]*Physics Department, The Technion, 32000 Haifa, Israel*
[3]*INAF – Osservatorio Astrofisico di Torino, Strada Osservatorio 20, I-10025 Pino Torinese, Italy*
[4]*School of Physics and Astronomy, Rochester Institute of Technology, 84 Lomb Memorial Drive, Rochester, NY 14623-5603, USA*

Accepted 2016 February 4. Received 2016 February 4; in original form 2015 December 16

ABSTRACT

Several studies indicate that radio-loud (RL) active galactic nuclei (AGNs) are produced only by the most massive black holes (BH), $M_{\rm BH} \sim 10^8$–10^{10} M$_\odot$. This idea has been challenged by the discovery of RL Narrow Line Seyfert 1 (RL NLSy1), having estimated masses of $M_{\rm BH} \sim 10^6$–10^7 M$_\odot$. However, these low $M_{\rm BH}$ estimates might be due to projection effects. Spectropolarimetry allows us to test this possibility by looking at RL NLSy1s under a different perspective, i.e. from the viewing angle of the scattering material. We here report the results of a pilot study of Very Large Telescope spectropolarimetric observations of the RL NLSy1 PKS 2004−447. Its polarization properties are remarkably well reproduced by models in which the scattering occurs in an equatorial structure surrounding its broad-line region, seen close to face-on. In particular, we detect a polarized Hα line with a width of ∼9000 km s^{-1}, ∼6 times broader than the width seen in direct light. This corresponds to a revised estimate of $M_{\rm BH} \sim 6 \times 10^8$ M$_\odot$, well within the typical range of RL AGN. The double-peaked polarized broad Hα profile of the target suggests that the rare combination of the orientation effects and a broad line region dominated by the rotation might account for this class of objects, casting doubts on the virial estimates of BH mass for type-I AGN.

Key words: line: profiles – polarization – galaxies: active – galaxies: individual: PKS 2004 −447 – galaxies: jet.

1 INTRODUCTION

Narrow line Seyfert 1 (NLSy1) are active galactic nuclei (AGNs) in which the width of the broad emission lines is smaller than 2000 km s^{-1} and showing a [O III]/Hβ ratio smaller than 3 (Osterbrock & Pogge 1985). The estimated masses of their black holes (BHs), based on the full width at half-maximum (FWHM) of the broad-line region (BLR) lines and the continuum luminosity (e.g. Kaspi et al. 2000), are typically $M_{\rm BH} \sim 10^6$–10^7 M$_\odot$. A recent surprising result is the discovery of a sub-population of NLSy1s with characteristics typical of radio-loud (RL) AGN (e.g. Zhou et al. 2006; Yuan et al. 2008; D'Ammando et al. 2012; Foschini et al. 2012; Angelakis et al. 2015). In contrast, classical RL AGN are invariably associated with the most massive BH, with $M_{\rm BH} > 10^8$ M$_\odot$ (e.g. Laor 2000; Baldi & Capetti 2010; Chiaberge & Marconi 2011). This result suggests two possible interpretations: RL NLSy1s correspond to a fundamentally different mechanism for the formation of relativistic jets (e.g. Komossa et al. 2006; Gu et al. 2015). Alternatively, the $M_{\rm BH}$ estimates in RL NLSy1s are underestimated.

One possibility to account for their 'narrow' broad Balmer lines is that the BLR clouds in RL NLSy1s are mostly confined in a rotating disc. When such a disc is seen at a small angle with respect to our line of sight, projection effects reduce the observed line width leading to an underestimate of the BH mass values. Several indications favour a pole-on orientation for RL NLSy1, including rapid variability, one-sided radio jets, and extreme γ-rays luminosity, all requiring high Doppler boosting typical of relativistic jets observed at a small angle from their axis (e.g. Komossa et al. 2006, 2015; Doi et al. 2007). The presence of a dependence of the BLR line width with orientation is already well established for RL AGN (e.g. Wills & Browne 1986; Fine, Jarvis & Mauch 2011; Runnoe et al. 2013), in the sense that objects observed at smaller angles from their jet axis show narrower lines. RL NLSy1s might be extreme examples of such an effect.

Spectropolarimetry is a unique tool to probe the geometry of AGN. Among the many results obtained with this technique there is the Unified Model, proposed to account for the polarized broad lines

★ E-mail: R.Baldi@soton.ac.uk

seen in objects showing only narrow lines in direct light (Antonucci 1983; Miller & Antonucci 1983; Antonucci & Miller 1985). This is due to the scattering of the light of a hidden BLR into our line of sight, leading to a polarized emission. Also in the case of NLSy1s spectropolarimetry enables us to observe their BLR under a different perspective. For example, a scattering region located in the AGN equatorial plane will see the full rotation amplitude of the BLR and the light reflected (and thence polarized) will show the intrinsic value of the BLR line width. The presence of scattering material in the equatorial plane is supported by the polarization properties of the majority of type 1 AGN, where the polarization is parallel to the radio axis (while in type 2 is usually perpendicular) and the polarization angle rotates within the broad line. This behaviour is well reproduced by a geometry in which the scatterers are mainly located in an annulus immediately surrounding the BLR (Smith et al. 2004, 2005).

Several spectropolarimetric studies of NLSy1s has been performed (e.g. Goodrich 1989; Breeveld & Puchnarewicz 1998; Kay et al. 1999; Robinson et al. 2011) but none of them included RL objects of this class.

We here present the results of a pilot study of Very Large Telescope (VLT) spectropolarimetric observations of an RL NLSy1, namely PKS 2004−447, at $z = 0.240$. We selected it because of its detection (and variability) in γ-rays by *Fermi* (Abdo et al. 2009; Calderone et al. 2011), the clearest evidence for the presence of an RL nucleus. Among the few RL NLSy1s with a γ-rays detection, PKS 2004−447 is the only source in the Southern sky at sufficiently low redshift that the Hα line falls within an optical spectrum.

PKS 2004−447 is a compact steep-spectrum radio source, with a core-jet morphology on pc scales (Schulz et al. 2015), and its broad-band spectral energy distribution (SED) shows the double-humped shape typical of blazars (Gallo et al. 2006; Orienti et al. 2015). The FWHM of its broad Hβ line is 1447 km s^{-1} (Oshlack, Webster & Whiting 2001), within the upper limit considered to define NLSy1s; the corresponding BH mass is $\sim 5 \times 10^6$ M$_\odot$. The strength of the Fe II lines is low (with an equivalent width for the whole Fe II complex in the region 5050–5450 Å smaller than 10 Å) with respect to what is usually found in NLSy1s (Osterbrock & Pogge 1987; Boroson & Green 1992); conversely, the ratio [O III]/H$\beta = 1.6$ conforms with typical values of NLSy1. Oshlack et al. (2001) also estimated a radio-loudness $R = f_{4.85\ \mathrm{GHz}}/f_B \sim 1710$–$6320$ (depending on the value used for the optical magnitude) well above the threshold for RL AGN ($R > 10$; Kellermann et al. 1989).

A cosmology with $H_0 = 72$ km s^{-1} Mpc^{-1}, $\Omega_\mathrm{m} = 0.30$, and $\Omega_\Lambda = 0.70$ is assumed, corresponding to a luminosity distance for PKS 2004−447 of 1.17 Gpc.

2 OBSERVATIONS AND DATA ANALYSIS

PKS 2004−447 was observed in spectropolarimetric mode with the FORS2 mounted at the UT1 telescope of the 8.2-m European Southern Observatory (ESO) VLT on 2015 May 11 and 23 with a seeing better than <1 arcsec. The observations were obtained with the GRISM-300I, providing a spectral resolution of $R \sim 660$ at 8600 Å, used in combination with the blocking filter OG590. The 1 arcsec wide slit was oriented along the parallactic angle and the multi-object spectropolarimetry observation was performed with a 2048 × 2048 pixel CCD with a spatial resolution of 0.126 arcsec pixel^{-1}.

The measurements at two retarder angles are sufficient to calculate the linear Stokes parameters. However, in order to reduce instrumental issues (Patat & Romaniello 2006), we used four half-wave plate angles (0, 22.5, 45, and 67.5 deg) for our observations. This strategy was repeated four times in separated observing blocks. Each block consists of four spectra (split in two exposures for cosmic rays removal) with an exposure time of 10.25 min, with the half-plate oriented at the four position angles. Since the observation of the first night failed, we used only three observing blocks, for a total on-source time of ∼2 h.

The data were analysed by using the standard VLT pipeline with the ESO Reflex workflow (Hook et al. 2008). The frames were first bias-subtracted and then flat-fielded using lamp flats. After removing cosmic ray events, the different exposures for the four half-wave plate positions were combined for each observing block. One-dimensional spectra, with identical aperture widths for the ordinary (o) and extraordinary (e) rays for each of the four half-wave plate orientations, were then extracted (from 12 pixels corresponding to 1.5 arcsec). The wavelength calibration was performed using standard arc lamps. The o and e rays were resampled to the same linear spectral dispersion and combined (by including data for all three observing blocks) to determine the three Stokes parameters I, Q, and U (as well as the associated uncertainties) using the procedures described by Cohen et al. (1995) and Vernet et al. (2001). No flux calibration was performed.

3 RESULTS

The total intensity spectrum is shown in the top panel of Fig. 1. It shows a broad Hα line, blended with [N II] λλ6548,84 doublet, with an FWHM ∼ 1500 km s^{-1}, consistent with the Hβ width measured by Oshlack et al. (2001). Fainter emission lines are also seen, namely the [O I] λλ6300,64 and [S II] λλ6716,31 doublets, superposed on to a featureless continuum. The signal-to-noise ratio of the total intensity spectrum is ∼150 per pixel on the continuum and it reaches ∼500 on the Hα.

Since the polarization of the target turns out to be extremely low (see below for the details) the spectra were rebinned in order to obtain, where possible, statistically significant polarization measurements. The bin sizes used are broader in the continuum far from the spectral regions of interest (i.e. the broad Hα line), where bin sizes of either 150 and 250 Å, were used. A finer binning (15 Å) is maintained across the Hα, while the integration regions are between 30 and 50Å on its wings. In Fig. 1, we present the resulting Stokes parameters Q and U, the polarized spectrum $I_\mathrm{P} = (Q^2 + U^2)^{1/2}$, the corresponding degree of polarization $P = I_\mathrm{P}/I$, and the polarization position angle, PA (measured counterclockwise starting from north). The PA is plotted only in the regions of significant polarization.

The overall polarization level of this source (integrated between 5404 and 7254 Å) is consistent with a null value, namely $P = 0.03 \pm 0.02$ per cent, despite the very high accuracy that can be reached with our data. The same result is obtained for the continuum emission. We measured it in two spectral regions ∼±500 Å far from the broad Hα (covering 5404–5904 and 6754–7254 Å, respectively) failing to detect any significant polarization.

The BLR seen in direct light does show a polarization of 0.0076 ± 0.0024 per cent integrated over the wavelength range 6534–6594 Å, with a polarization position angle of PA $= 32^\circ \pm 6^\circ$. While its polarization has a statistical significance of $\sim 3\sigma$, we cannot exclude that we are seeing a minimal residual instrumental polarization. Certainly, this measurement can be adopted as a firm upper limit to any instrumental effect.

The only reliable polarized signal found in PKS 2004−447 is seen on both sides of the broad Hα. We measure a degree of polarization

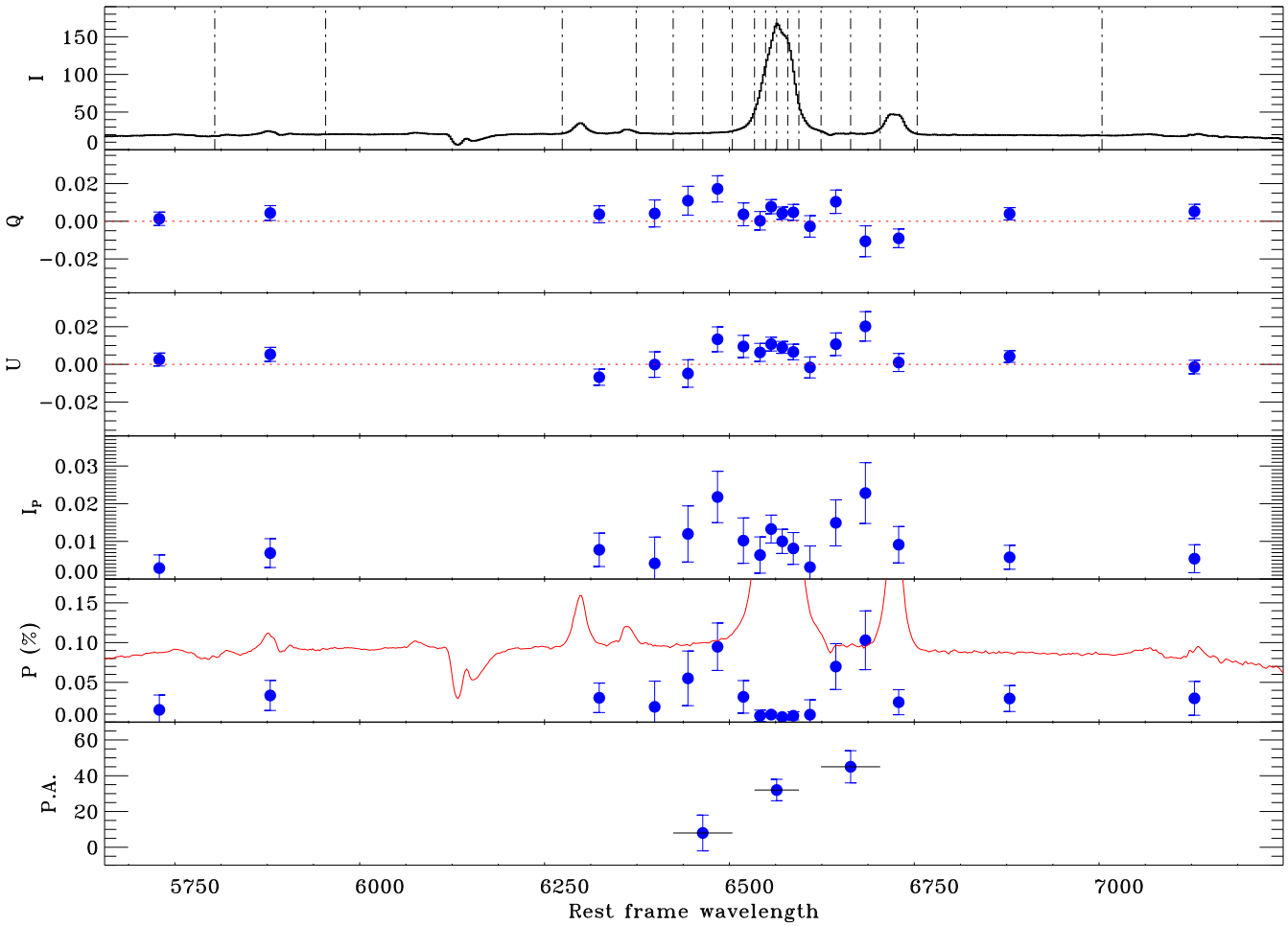

Figure 1. Top three panels: Stokes parameters of the PKS 2004−447 spectrum. Wavelengths are shown in rest frame in Å, fluxes are in arbitrary units because no flux calibration was performed. The vertical dashed lines mark the boundaries of the regions used for the spectral rebinning. Bottom three panels: polarized flux, percentage of polarization (with overplotted, in red, the total intensity spectrum), and polarization position angle. The PA is reported only in the regions of reliable polarization, see text for details. The region around ∼6100 Å has been flagged due to the residuals related to the presence of a telluric absorption feature and of bright sky lines.

of $P = 0.066 \pm 0.023$ per cent at PA $= 8^\circ \pm 10^\circ$ on the blue side (for $6424 < \lambda < 6504$ Å) and $P = 0.070 \pm 0.023$ per cent at PA $= 45^\circ \pm 9^\circ$ on the red side (for $6624 < \lambda < 6704$ Å).

4 DISCUSSION

The spectropolarimetric observations show a broader polarized Hα with respect to what is seen in direct light. This is what is expected if we are seeing the Hα emission from a disc-like BLR reflected from a coplanar circumnuclear scattering region. Due to the location of the scatterers, they see the full BLR velocity field; thus the amplitude of the scattered (and thence polarized) broad line reflects the genuine gas motions close to the central BH. This confirms our suggestion that projection plays a fundamental role in RL NLSy1.

The polarization behaviour of PKS 2004−447 is in remarkable agreement with the results of the models of presented by Smith et al. (2005). They simulated the polarization properties of a rotating line-emitting disc (the BLR) surrounded by a coplanar scattering region. The main predictions are (i) the presence of polarization peaks in the line wings, (ii) a rotation of the polarization PA across the BLR, and (iii) a higher polarization in the line with respect to the continuum, all effects seen in the observed source.

In the equatorial scattering models, the polarization level decreases for sources seen at lower inclination. This is due to the cancellation between the polarization vectors produced in the different portions of the scattering region, which is more efficient for low-inclination angles (a null P value is predicted for an exact face-on orientation). Indeed, the measured percentage of polarization (∼0.07 per cent) is an order of magnitude smaller than usually observed in type I Seyfert (Smith et al. 2002), as expected for a source seen close to face-on. As discussed above, this is likely to be the case for our target.

Another signature of equatorial scattering is the angle swing across the Hα line. The PA of the continuum polarization defines the reference value, parallel to the projection of the symmetry axis. Across the polarized broad line, the PA rotates in opposite directions in the blue and red wings, with the largest deviations occurring just inside the peaks of polarization percentage. This feature is seen in PKS 2004−447 with a rotation of $37^\circ \pm 13^\circ$ from the blue to the red Hα wings. However, the non-detection of continuum polarization (that is indeed expected to be lower than on the line wings) does not allow us to trace fully the PA changes. Furthermore, the actual rotation across the line might be even larger considering the heavy smoothing of our data. None the less, the observed PA swing is

already larger than usually measured in Seyferts Is and indeed the models indicate that such effect is amplified for small inclinations, as in the case for our target.

With respect to the model predictions, we find a possible discrepancy, related to the relative PA of the BLR polarization and the radio jet that are expected to be parallel to each other. The BLR polarization angle, averaged over the two wings, is $27^\circ \pm 7^\circ$ while the radio jet is elongated in a general EW direction (Orienti et al. 2015). However, the jet is strongly bent, starting along PA $\sim -90^\circ$ out to $\sim$15 pc, where it curves northward by $\sim 45^\circ$. Large bends are commonly observed in blazar radio jets, often also associated with temporal changes of their orientation (Lister et al. 2013); this is due to projection effects that, in objects seen pole-on, amplify the intrinsic variation of the jet position angles. For such objects, it is difficult to establish in which direction the jet is actually pointing. Furthermore, Smith et al. (2004) noticed that Seyfert type 1 galaxies often show a similar perpendicular inclination between the radio and BLR position angles. They proposed that an asymmetry of the density distribution of the scattering region might account for such a configuration. For these reasons, the apparent offset between the position angles of the BLR polarization and the jet orientation found in PKS 2004−447 should not be considered as a strong shortcoming of the scattering model proposed.

According to the standard equatorial model of Smith et al. (2005, see their fig. 4), the separation between the peaks in the percentage of polarization corresponds to the intrinsic (i.e. corrected for projection) width of the broad Hα. In our case, although, due to the low-polarization level, this measurement has a relatively large uncertainty. In these spectral regions, the bin sizes are of 30–40 Å; by adopting these values as errors for the location of the two polarization peaks, they turn out to be separated by 200 ± 50 Å, corresponding to a velocity width of $9100 \pm 2300\,\mathrm{km\,s^{-1}}$, a value within the range covered by the broad Balmer lines in RL AGN (Wills & Browne 1986; Runnoe et al. 2013).

The broadening with respect to what is seen in direct light is dramatic. As a consequence, the BH mass estimate is increased by a factor $\sim$30 with respect to the estimate obtained from the total intensity spectrum. Given the continuum luminosity of $L_{5100} \sim 1.25 \times 10^{44}\,\mathrm{erg\,s^{-1}\,cm^{-2}\,\text{Å}^{-1}}$ (Gallo et al. 2006), the corresponding BLR size is $\sim$38 light days (Bentz et al. 2013). By adopting the width of the polarized broad Hα,[1] we derive a mass of $M_{\rm BH} \sim 6 \times 10^8\,\mathrm{M_\odot}$. This revised estimate falls in the range of the BH masses typical of RL AGN (Chiaberge & Marconi 2011).

Calderone et al. (2013) reached a similar conclusion from a method to estimate BH masses which relies on the modelling of optical and ultraviolet data of 23 RL NLSy1 with an accretion disc spectrum. Their study returns values of $M_{\rm BH}$ consistently larger than $\gtrsim 10^8\,\mathrm{M_\odot}$.

The results obtained from our study lead us to consider the further issue of why RL NLSy1s are so rare. In principle, flat spectrum radio-quasars (FSRQ), objects known to be observed at small inclinations, should also show narrow BLR profiles. While indeed the FWHM of the broad emission lines in FSRQ is reduced with respect to the general population of QSOs, only a small minority of them have a width $<2000\,\mathrm{km\,s^{-1}}$ (Shaw et al. 2012). This implies that projection effects are not as effective in these sources; this is expected when non-rotational motions, such as e.g. those associated with an outflow contribute significantly to the BLR velocity field or when the BLR is characterized by a large vertical thickness. It appears that a combination of face-on inclination and a BLR dominated by rotation (in the Balmer lines) are probably required to produce an RL NLSy1.

The dominance of rotation was proposed by Eracleous & Halpern (2003) to account for the BLR properties of another class of objects, the so-called double-humped AGN (DH-AGN) in which the broad line profiles show two well-separated emission peaks; DH-AGN constitute $\sim$20 per cent of RL AGN for $z < 0.4$. In most cases the 'double-humped' profiles can be described very well by models attributing the emission to a flattened rotating BLR (for a review see Eracleous, Lewis & Flohic 2009). By extrapolating the results obtained for PKS 2004−447, we speculate that RL NLSy1s are the result of the rare combination of an intrinsically DH-AGN that is seen nearly face-on.

Regardless of the proposed identification of the parent population (i.e. of the objects with the same intrinsic properties but observed at larger inclinations), the expected broadening of the BLR for RL NLSy1s seen at large angles is an effect that should be included in the search for their misoriented counterparts (see e.g. Berton et al. 2015).

5 SUMMARY AND CONCLUSIONS

The spectropolarimetric observations of the RL NLSy1s PKS 2004−447 show the presence of two peaks of polarized flux separated by $\sim$250 Å flanking the Hα seen in the total intensity spectrum. The overall polarization properties of this source are remarkably well reproduced as due to the scattering of the BLR emission from an equatorial structure seen at very small inclination from its axis. In particular, this model predicts the extremely low level of polarization ($\sim$0.07 per cent) and the change of position angle across the broad Hα. In this situation, the scattering material, from its vantage point, sees the full velocity field of the BLR, removing the effects of projection. The separation between the polarization peaks is a direct measure of its intrinsic width, that results in $\sim 9000\,\mathrm{km\,s^{-1}}$. By adopting the standard scaling relations, we derive a BH mass of $M_{\rm BH} \sim 6 \times 10^8\,\mathrm{M_\odot}$. This revised estimate strengthens the conclusion that RL AGN are only associated with very massive BHs ($\gtrsim 10^8\,\mathrm{M_\odot}$).

It must be stressed that our results do not apply to the class of NLSy1s as a whole. In fact, we are interpreting the observations of an object that was selected among the small sub-class of RL sources, while the vast majority of NLSy1s are radio quiet (RQ). In particular, the large BH mass estimated for PKS 2004−447 does not necessarily conflict with the suggestion, based on various properties of NLSy1, that they are generally associated with small BHs accreting at high rates (e.g. Valencia-S. et al. 2012). Indeed, previous spectropolarimetric studies of RQ NLSy1s (e.g. Goodrich 1989) do not show an Hα broadening in polarized light. These latter results apparently contrast with the suggestion by Decarli et al. (2008) that the properties of NLSy1 can be accounted for with a preferential face-on orientation. Furthermore, although PKS 2004−447 qualifies as an NLSy1s based on its main optical properties (broad emission line width and [O III]/Hβ ratio), it shows rather different characteristics (such as its broad-band SED and the strength of the Fe II lines) with respect to what is typical for NLSy1. We concur with Oshlack et al. (2001), who argue that since NLSy1s are defined by phenomenological measurements, rather than a specific physical model, it is possible that more than one physical mechanism will produce the defining parameters. In particular, the low widths of

[1] We assumed a geometric factor $f = 1$ in the virial formula to account for the edge-on location of the scatterers.

their broad lines is not generally due to projection. Our spectropolarimetry results strongly suggest that this is, in fact, the case for at least one RL NLSy1, although, clearly, more spectropolarimetric observations will be required to determine if this conclusion holds for the RL sub-population in general.

On the other hand, not all RL AGN seen at small inclinations have small broad emission line widths; indeed only a minority of them show values smaller than the threshold of 2000 km s^{-1} required for a classification as NLSy1. This indicates that a further ingredient, other than orientation, is needed to produce an RL NLSy1. In particular, the dependence of the broad emission line width with orientation is maximized when its velocity field is dominated by rotation. We speculate that the parent population of RL NLSy1s is represented by sub-class of the so called double humped AGN; in these objects the lines profiles can be reproduced accurately by models attributing the emission to a flattened rotating BLR. We argued that RL NLSy1s are the result of the rare combination of an intrinsically DH-AGN that is seen nearly face-on.

Our results also suggest that orientation effects might play an important role in the BH estimates based on the virial method not only for NLSy1 but more in general for AGN and particularly for those seen close to face-on. For example, in FSRQ the median angle formed by the jet with the line of sight is $\sim 3^{\circ}$ (Savolainen et al. 2010) and this reduces the rotation amplitude by a factor of $\sim$20 with respect to its intrinsic value in case of a disc-like geometry. Furthermore, since disc winds seem to be important for gas dynamics and ubiquitous in AGN (e.g. Veilleux, Cecil & Bland-Hawthorn 2005), any outflowing component might represent the dominant source of observed line broadening in these AGN. These factors cast doubts on the reliability of virial estimates of their BH masses.

ACKNOWLEDGEMENTS

RDB is grateful to S. Raimundo for the discussion which inspired this work. We thank the referee for constructive comments/suggestions to improve the manuscript. EB received funding from the European Unions Horizon 2020 research and innovation programme under the Marie Sklodowska-Curie grant agreement no. 655324, and from the I-CORE program of the Planning and Budgeting Committee (grant number 1937/12).

REFERENCES

Abdo A. A. et al., 2009, ApJ, 707, L142
Angelakis E. et al., 2015, A&A, 575, A55
Antonucci R. R. J., 1983, Nature, 303, 158
Antonucci R. R. J., Miller J. S., 1985, ApJ, 297, 621
Baldi R. D., Capetti A., 2010, A&A, 519, A48
Bentz M. C. et al., 2013, ApJ, 767, 149
Berton M. et al., 2015, A&A, 578, A28
Boroson T. A., Green R. F., 1992, ApJS, 80, 109
Breeveld A. A., Puchnarewicz E. M., 1998, MNRAS, 295, 568
Calderone G., Foschini L., Ghisellini G., Colpi M., Maraschi L., Tavecchio F., Decarli R., Tagliaferri G., 2011, MNRAS, 413, 2365
Calderone G., Ghisellini G., Colpi M., Dotti M., 2013, MNRAS, 431, 210
Chiaberge M., Marconi A., 2011, MNRAS, 416, 917
Cohen M. H., Ogle P. M., Tran H. D., Vermeulen R. C., Miller J. S., Goodrich R. W., Martel A. R., 1995, ApJ, 448, L77
D'Ammando F. et al., 2012, MNRAS, 426, 317
Decarli R., Dotti M., Fontana M., Haardt F., 2008, MNRAS, 386, L15
Doi A. et al., 2007, PASJ, 59, 703
Eracleous M., Halpern J. P., 2003, ApJ, 599, 886
Eracleous M., Lewis K. T., Flohic H. M. L. G., 2009, New Astron. Rev., 53, 133
Fine S., Jarvis M. J., Mauch T., 2011, MNRAS, 412, 213
Foschini L. et al., 2012, A&A, 548, A106
Gallo L. C. et al., 2006, MNRAS, 370, 245
Goodrich R. W., 1989, ApJ, 342, 224
Gu M., Chen Y., Komossa S., Yuan W., Shen Z.-Q., Wajima K., Zhou H., Zensus J. A., 2015, ApJS, 221, 3
Hook R. et al., 2008, in Argyle R. W., Bunclark P. S., Lewis J. R., eds, ASP Conf. Ser. Vol. 394, Astronomical Data Analysis Software and Systems XVII. Astron. Soc. Pac., San Francisco, p. 638
Kaspi S., Smith P. S., Netzer H., Maoz D., Jannuzi B. T., Giveon U., 2000, ApJ, 533, 631
Kay L. E., Magalhães A. M., Elizalde F., Rodrigues C., 1999, ApJ, 518, 219
Kellermann K. I., Sramek R., Schmidt M., Shaffer D. B., Green R., 1989, AJ, 98, 1195
Komossa S., Voges W., Xu D., Mathur S., Adorf H.-M., Lemson G., Duschl W. J., Grupe D., 2006, AJ, 132, 531
Komossa S. et al., 2015, A&A, 574, A121
Laor A., 2000, ApJ, 543, L111
Lister M. L. et al., 2013, AJ, 146, 120
Miller J. S., Antonucci R. R. J., 1983, ApJ, 271, L7
Orienti M., D'Ammando F., Larsson J., Finke J., Giroletti M., Dallacasa D., Isacsson T., Stoby Hoglund J., 2015, MNRAS, 453, 4037
Oshlack A. Y. K. N., Webster R. L., Whiting M. T., 2001, ApJ, 558, 578
Osterbrock D. E., Pogge R. W., 1985, ApJ, 297, 166
Osterbrock D. E., Pogge R. W., 1987, ApJ, 323, 108
Patat F., Romaniello M., 2006, PASP, 118, 146
Robinson A., Young S., Axon D. J., Smith J. E., 2011, in Bastien P., Manset N., Clemens D. P., St-Louis N., eds, ASP Conf. Ser. Vol. 449, Astronomical Polarimetry 2008: Science from Small to Large Telescopes. Astron Soc. Pac., San Francisco, p. 431
Runnoe J. C., Brotherton M. S., Shang Z., Wills B. J., DiPompeo M. A., 2013, MNRAS, 429, 135
Savolainen T., Homan D. C., Hovatta T., Kadler M., Kovalev Y. Y., Lister M. L., Ros E., Zensus J. A., 2010, A&A, 512, A24
Schulz R. et al., 2015, A&A, preprint (arXiv:1511.02631)
Shaw M. S. et al., 2012, ApJ, 748, 49
Smith J. E., Young S., Robinson A., Corbett E. A., Giannuzzo M. E., Axon D. J., Hough J. H., 2002, MNRAS, 335, 773
Smith J. E., Robinson A., Alexander D. M., Young S., Axon D. J., Corbett E. A., 2004, MNRAS, 350, 140
Smith J. E., Robinson A., Young S., Axon D. J., Corbett E. A., 2005, MNRAS, 359, 846
Valencia-S. M. et al., 2012, Proc. Sci., Nuclei of Seyfert galaxies and QSOs – Central Engine & Conditions of Star Formation. Max-Planck-Insitut für Radioastronomie, Bonn, p. 17
Veilleux S., Cecil G., Bland-Hawthorn J., 2005, ARA&A, 43, 769
Vernet J., Fosbury R. A. E., Villar-Martín M., Cohen M. H., Cimatti A., di Serego Alighieri S., Goodrich R. W., 2001, A&A, 366, 7
Wills B. J., Browne I. W. A., 1986, ApJ, 302, 56
Yuan W., Zhou H. Y., Komossa S., Dong X. B., Wang T. G., Lu H. L., Bai J. M., 2008, ApJ, 685, 801
Zhou H., Wang T., Yuan W., Lu H., Dong X., Wang J., Lu Y., 2006, ApJS, 166, 128

This paper has been typeset from a TEX/LATEX file prepared by the author.